Institute of Pharmaceutical Technology[1], Johann Wolfgang Goethe University, Frankfurt am Main, Germany; Nanosystem Ltd.[2], Moscow, Russia

Development of nanoparticle-bound arylsulfatase B for enzyme replacement therapy of mucopolysaccharidosis VI

A. Mühlstein[1], S. Gelperina[2], J. Kreuter[1]

Received September 11, 2012, accepted December 11, 2012

Prof. Dr. Jörg Kreuter, Institut für Pharmazeutische Technologie, Johann Wolfgang Goethe-Universität, Max-von-Laue Str. 9, 60438 Frankfurt am Main, Germany
kreuter@em.uni-frankfurt.de

Dedicated to Prof. Dr. Theo Dingermann, Frankfurt, on the occasion of his 65th birthday.

Pharmazie 68: 549–554 (2013) *doi: 10.1691/ph.2013.6502*

Lysosomal storage disorders like mucopolysaccharidosis (MPS) VI are rare diseases with a lack of well-suited treatments. Even though an enzyme replacement therapy (ERT) of recombinant arylsulfatase B (ASB) is available for MPS VI, the administration cannot positively affect the neurologic manifestations such as spinal cord compression. Since nanoparticles (NP) have shown to be effective drug carriers, the feasibility of arylsulfatase B adsorption onto poly(butyl cyanoacrylate) (PBCA) nanoparticles was investigated in this study. In order to advance the ERT of ASB, the adsorption of the latter on the surface of PBCA NP as well as *in vitro* release in serum was investigated. With alteration of parameters like temperature, incubation time, pH, and enzyme amount, the adsorption process revealed to be stable with a maximum capacity of 67 μg/mg NP at a pH of 6.3. *In vitro* release experiments demonstrated that the adsorption is stable for at least 60 minutes in human blood serum, indicating that the ASB-loaded PBCA nanoparticles represent a promising candidate for ERT of MPS VI.

1. Introduction

Lysosomal storage disorders (LSD) are rare genetic diseases that are caused by a deficiency of one or more degradation enzymes essential for normal cell metabolism. In mucopolysaccharidosis type VI (MPS VI), the lack of *N*-acetylgalactosamine-4-sulfatase (arylsulfatase B, Naglazyme®, BioMarin Europe Ltd.) leads to the accumulation of its substrate, dermatan sulfate and chondroitin 4-sulfate, which results in severe skeletal abnormalities, cardiac valve disease, reduced pulmonary function, and other malfunctions including the CNS involvement. A gradual thickening of the *dura mater* and their supporting structures are considered to be the cause for the elevation of the pressure on the spinal cord, which leads to severe leg paresis of MPS VI patients (Auclair et al. 2010).

The best treatment option for MPS VI is enzyme replacement therapy (ERT) using human recombinant arylsulfatase B that became available recently. However, although ERT certainly is a real breakthrough in the treatment of LSD, it has serious limitations. For example, intravenously administered lysosomal enzymes are rapidly removed from the circulation by a receptor-mediated process. In addition, the transfer of enzyme from the circulation to the brain is limited because of the blood–brain barrier (BBB) (Fuller et al. 2005; Wraith 2006). At present, only direct injection of enzyme into the cerebrospinal fluid has been shown to significantly reduce lysosomal storage in the *dura mater* of MPS VI cats (Auclair et al. 2010, 2012) and MPS-I dogs (Kakkis et al. 2004). Therefore, a suitable carrier system that enhances the brain uptake of the lysosomal enzyme would considerably advance its clinical usefulness.

The objective of the present study was to evaluate the possibility to bind arylsulfatase B (ASB) to poly(butyl cyanoacrylate) (PBCA) nanoparticles (NPs). Previous investigations showed a transport of a variety of drugs like dalargin, loperamide, doxorubicin, and even larger proteins such as nerve growth factor (NGF) over the blood-brain barrier (BBB) using nanoparticles (Alyautdin et al. 1995, 1997, 1998; Kurakhmaeva et al. 2009; Steiniger et al. 2004). An analysis of the nanoparticle transport mechanism by transmission electron microscopy indicated that the cell uptake appears to be receptor-mediated endocytosis followed by transcytosis (Zensi et al. 2009). No opening of the tight junctions was observed after i.v. injection of the particles. Due to the coating of the nanoparticles with polysorbate 80 or poloxamer 188 depending on the core polymer – apolipoproteins A-1 and/or E are adsorbed from the blood on to the particle surface after i.v. injection. These apolipoproteins then mediate the interaction of the particle with LDL or scavenger receptors on the brain capillary endothelial cells followed by the brain uptake processes. Likewise, the covalent attachment of these apolipoproteins or of transferrin, insulin, or antibodies against the transferrin or insulin receptors also enables a similar nanoparticle-mediated drug transport across the BBB (Kreuter et al. 2002; Michaelis et al. 2006). Nanoparticles also may be suitable for delivery to bones (Salerno et al. 2010). This finding initiated the attempt to adsorb ASB onto the PBCA NP surface to improve the efficacy of ASB ERT.

2. Investigations, results and discussion

2.1. Theoretical considerations of drug loading

In order to estimate the theoretically adsorbable amount of ASB onto the nanoparticle surface, calculations of the free NP sur-

face assuming a spherical shape and the adsorption of ASB as a monolayer were performed. The adsorbable number of ASB molecules per one nanoparticle (N_{ASB}) can be calculated as follows Eq. (1):

$$N_{ASB} = \frac{4\pi r^2}{S_{ASB}} \quad (1)$$

where r is the radius of one nanoparticle, and S_{ASB} the area occupied by one ASB molecule on nanoparticle surface.
Then the maximal amount of adsorbed ASB (M_{max}) per milliliter of NP suspension (10 mg/ml) can be calculated as:

$$M_{\max} = \frac{MM_{ASB} \cdot N_{ASB}}{N_A} \cdot \frac{C_{NP}}{\frac{4}{3}\pi r^3 \cdot d_{NP}} \quad (2)$$

where MM_{ASB}, is the molecular mass of ASB, N_A, the Avogadro constant, C_{NP} the concentration of NP (10 mg/ml), and d_{Np} the density of NP (1000 mg/cm^3).
Eq. (2) can be simplified as follows:

$$M_{\max} = \frac{MM_{ASB} \cdot C_{NP} \cdot 3}{N_A \cdot S_{ASB} \cdot d_{NP} \cdot r} \quad (3)$$

The dimensions of the ASB molecule have not been reported to our knowledge; however, it is known that ASB exists in the monomeric form with a molecular mass of 57 kDa (Gibson et al. 1987) and is homologous to another lysosomal enzyme, arylsulfatase A (Yaghootfam et al. 2003). Therefore, in the present study the dimensions of the monomeric unit of the arylsulfatase A assuming a hat-like molecululular structure with a base of 70 Å x 45 Å and the height of 50 Å was used for the calculation (Lukatela et al. 1998). Provided that the average diameter of the nanoparticle is 150 nm, its surface area is: $S_{NP} = 4\ \pi r^2 = 70690\ nm^2$. Finally, for the concentration of the nanoparticles of $C_{NP} = 20$ mg/ml and an approximate density of $d_{Np} = 1000$ mg/cm^3 (Kreuter 1983), a maximal adsorbable amount of ASB per 1 milligram of PBCA NP is equal to 120 μg Eq. (3).

2.2. Determination of ASB loading to PBCA NP

The amount of the ASB adsorbed to the particles was determined indirectly as a difference between the amount initially added to the particle suspension and the amount of free enzyme. For this purpose the nanoparticles were separated by centrifugation, and then the amount of free enzyme in the supernatant was measured by size exclusion chromatography (SEC) and specific activity assay using p-nitrocatechol sulphate (pNCS) as substrate (Baum et al. 1959). For validating and assessing the accuracy of these assays mass calibration and spike-and-recovery experiments were performed.
The pNCS assay reproducibly showed a linear dependence between ASB absorption and concentration in the range of 0-6 μg/ml (data not shown) (p = 0.95; n = 6; Sr = 1.15 %). As revealed in the preliminary experiments, the PBCA NPs do not interfere with the accuracy of the pNCS assay. The NP controls showed no detectable absorbance. The t-test of the pNCS spike-and-recovery experiment (p = 0.209) showed no statistically significant difference between both groups.
SEC is an optimal method for ASB determination in a concentration range of 20 to 3000 μg/ml with a detection limit of 10 μg/ml and a high precision (P = 0.95; n = 6; Sr = 2.2 %). the NPs had to be removed from the sample for SEC analysis.

Table 1: Physicochemical parameters of poly(butyl cyanoacrylate) nanoparticles (n = 3; mean ± S.D.)

Particle size (nm)	166 ± 16
Polydispersity index (0–1.0)	0.201 ± 0.02
Zeta potential (mV)	–4.4 ± 2.6
Particle yield (mg/ml)	5.7 ± 0.1

2.3. Drug loading

The adsorption of drugs to the nanoparticle surface may depend on a number of parameters (Richardson and Meakin 1974). Two different stabilizers were used for the emulsion stabilisation during the polymerisation process: poloxamer 188 (Pluronic® F 68) and dextran 70000. Dextran produced a considerable adsorption, whereas employment of poloxamer 188 resulted in a negligible ASB adsorption to the NP (Wang and Hanson 1988; Blanco and Alonso 1997; Nonckreman et al. 2010).
Therefore, in further experiments dextran 70000 was used as a particle stabilizer. The variations of temperature (4 °C and 21 °C) and incubation time (1, 2, 4, and 24 h) at a constant amount of ASB (0.5 mg/ml) and nanoparticles did not considerably influence the efficiency of the ASB binding indicating a robustness of the adsorption method. The maximal adsorption of 47 μg/mg NP was reached after one hour. A slight but statistically significant increase in nanoparticle binding was observed at 4 °C, therefore further experiments were performed at this temperature.
The influence of the ASB concentration and pH were also investigated. The obtained results were fitted to the Langmuir and Freundlich adsorption isotherm and compared to the above theoretical calculation. The physicochemical properties of the PBCA NPs are shown in Table 1. It was expected that with a negative surface charge of the NPs, the maximal drug binding capacity would increase due to electrostatic interactions. As the isoelectric point (pI) of ASB is 7.5 (Agogbua and Wynn 1976), the adsorption was performed at a pH range from 4.5 to 8.3, thus conferring a positive charge to the enzyme molecule. However, as shown in Fig. 1, the adsorption process appeared to be more dependent on the ASB concentration than on pH. At lower concentrations of the ASB nearly 100 % loading (pH 7.3) was achieved. The maximum of 64.5 μg ASB per 1 mg NPs was reached at pH 6.3 at the ASB concentration of 3000 μg/ml (Fig. 2). Since no significant differences occurred between 2500 μg/ml to 3000 μg/ml, a pH of 6.3 and an enzyme concentration of 2500 μg/ml was used for further experiments.

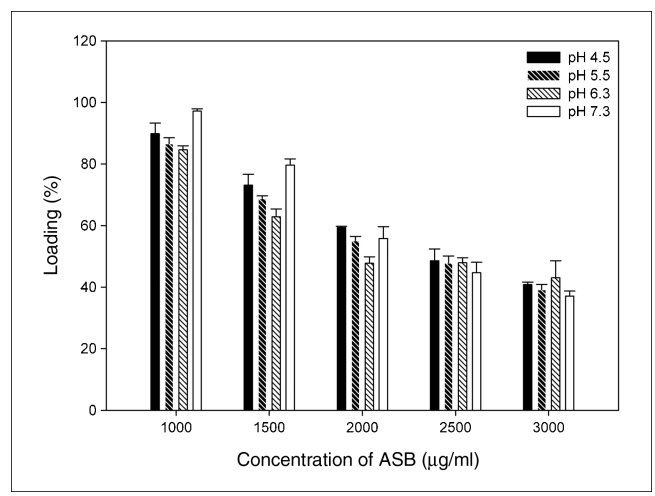

Fig. 1: Relative drug loading (%) of poly(butyl cyanoacrylate) nanoparticles at different pH values of adsorption media and different concentrations of ASB (n = 3; mean ± S.D.).

Table 2: Adsorption of arylsulfatase B to poly(butyl cyanoacrylate) nanoparticles at different pH fitted to linearised Freundlich and Langmuir model (n = 3; mean ± S.D.)

Isotherm model	pH	Correlation coefficient	Equation of the regression curve	n or q_{max} [µg/mg]
Langmuir model	4.5	0.9999	$c_{eq}/q = 0{,}016\ c_{eq} + 0{,}80$	$q_{max} = 62.5$
	5.5	0.9985	$c_{eq}/q = 0{,}016\ c_{eq} + 1{,}20$	$q_{max} = 62.5$
	6.3	0.9738	$c_{eq}/q = 0{,}015\ c_{eq} + 2{,}74$	$q_{max} = 66.7$
	7.3	0.9998	$c_{eq}/q = 0{,}018\ c_{eq} - 0{,}12$	$q_{max} = 55.6$
Freundlich model	4.5	0.9662	$\log(q) = 0{,}105\ \log(ceq) + 1{,}46$	n = 9,53
	5.5	0.9689	$\log(q) = 0{,}132\ \log(ceq) + 1{,}35$	n = 7,59
	6.3	0.7327	$\log(q) = 0{,}159\ \log(ceq) + 1{,}25$	n = 6,28
	7.3	0.4676	$\log(q) = 0{,}027\ \log(ceq) + 1{,}67$	n = 36,5

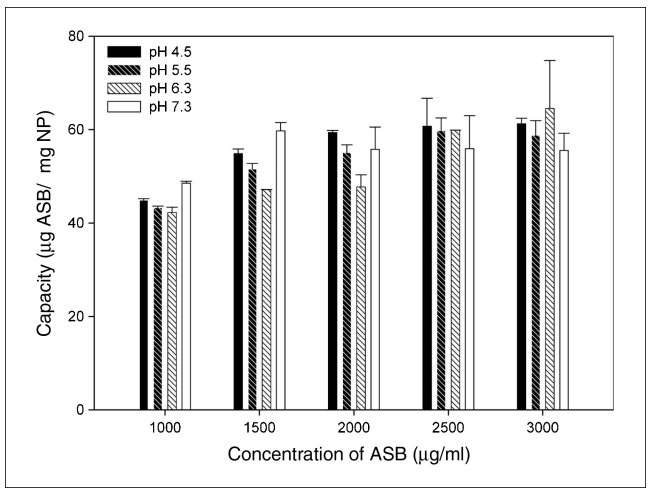

Fig. 2: Amount of drug loading (µg ASB/ mg NP) in poly(butyl cyanoacrylate) nanoparticles at different pH values of adsorption media and different concentrations of ASB (n = 3; mean ± S.D.).

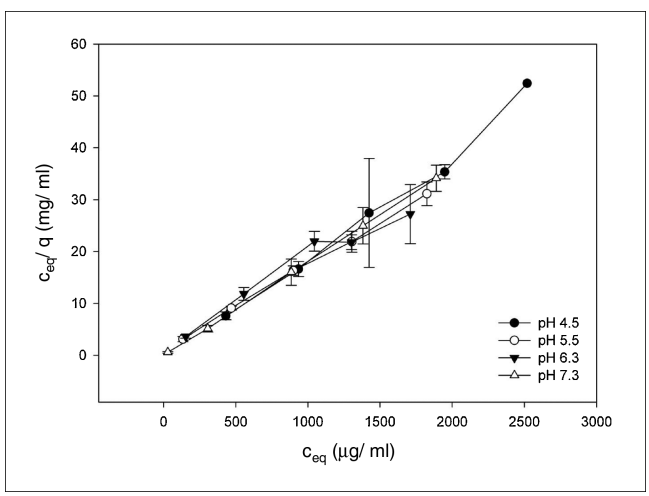

Fig. 3: Adsorption isotherms of ASB to poly(butyl cyanoacrylate) nanoparticles fitted to the linearised Langmuir model (n = 3; mean ± S. D.).

The data were fitted to Langmuir (Fig. 3) and Freundlich (Fig. 4) isotherms. The linearised adsorption correlated best with the Langmuir model (Langmuir 1916) ($R^2 = 0.999$ at pH 7.3) whereas according to the Freundlich isotherm the fit was only $R^2 = 0.467$ (Table 2). This result suggests that the ASB appears to adsorb as a monolayer to the surface of the PBCA nanoparticles.

For the calculation of the adsorption capacity q_{max} (Table 2), the obtained linear slope was used in Eq. (3), where q_{max} expresses the highest capacity of the surface to adsorb ASB which is dependent on the temperature, particle size, concentration, and pH. As shown in Table 2, the q_{max} increased with the raise of pH from 62.5 µg/mg until its maximum of 66.7 µg/mg at pH 6.3, whereas at pH 7.3 it decreases again to 55.6 µg/mg.

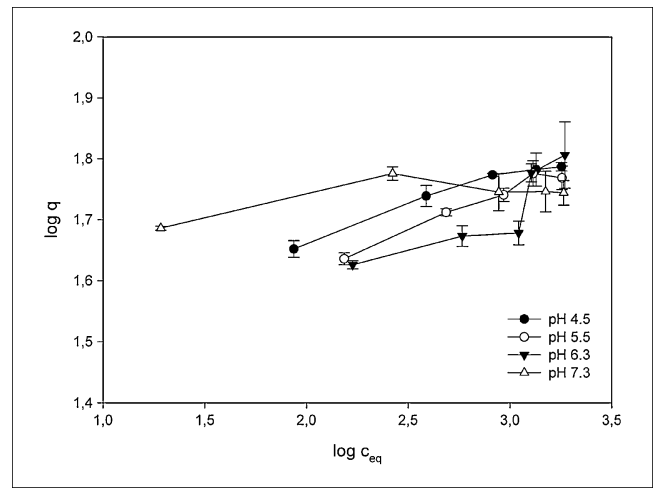

Fig. 4: Adsorption isotherms of ASB to poly(butyl cyanoacrylate) nanoparticles fitted to the linearised Freundlich model (n = 3; mean ± S. D.).

These findings allow the comparison of the experimental results with the theoretical adsorbable amount of ASB. Thus, for the 150-nm NPs the maximal adsorbable amount of ASB was calculated to be 120 µg/mg NP, whereas after fitting the experimental results to the Langmuir isotherm, a maximum of $q_{max} = 66.7$ µg/mg NP at pH 6.3 was found which is close to the maximal amount of 64.6 µg/mg polymer obtained experimentally. This can be caused by the form of ASB combined with a possible steric hindrance at the nanoparticle surface.

The scanning electron microscopy (SEM) pictures taken before and after drug loading (Fig. 5) did not reveal any change in the nanoparticle shape caused by the loading. However, on the surface of the loaded NPs (Fig. 5b) little round protrusions are visible. These structures have a size of about 7 - 10 nm. This size is very close to that of the ASB molecules (7.0 x 4.5 nm, Lukatela et al. 1998). However, as a severe *caveat*, it has to be considered that proteins may shrink during the preparation for the electron microscopy and due to the vacuum in the microscope. On the other hand, this size decrease of course is contrasted by the size increases caused by the gold sputtering. Nevertheless, the striking similarity of the sizes makes it very likely that these protrusions indeed represent ASB. Although these protrusions appear to be very regularly distributed, they do not connect but are separated by gaps of about the same size. These gaps, therefore, indicate that the adsorption does not follow pure Langmuirian adsorption processes, which may explain the differences in calculated maximal loading and experimental results. The reg-

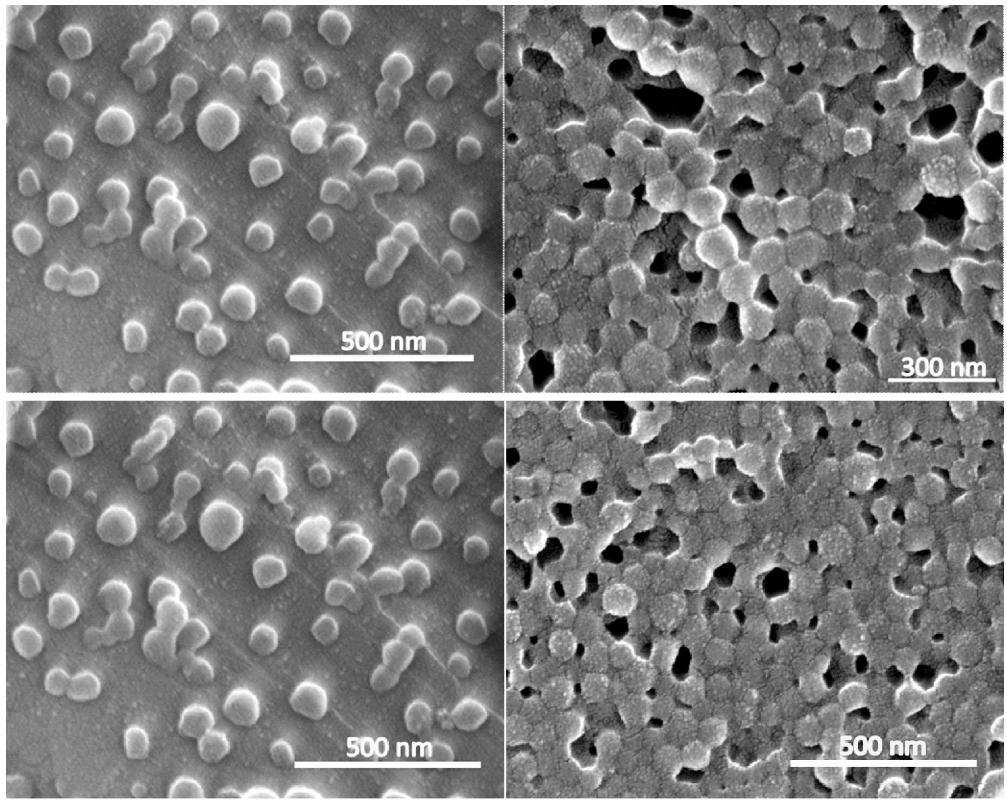

Fig. 5: Scanning electron microscopy pictures of poly(butyl cyanoacrylate) nanoparticles: empty particles (A) or particles loaded with ASB by adsorption (B). The agglomerations are an artifact due to sample preparation. Fig. 5B top shows the protrusions caused by the ASB at a higher magnification.

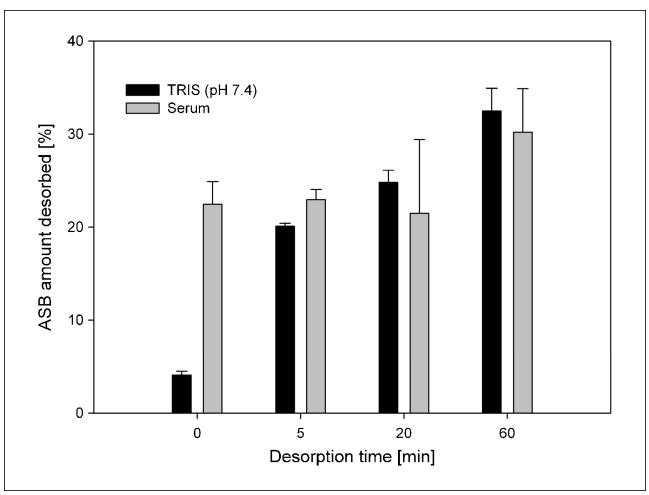

Fig. 6: Desorption of ASB from poly(butyl cyanoacrylate) nanoparticles in different media at 37 °C (n = 3; mean ± S.D.).

ular distribution on the other hand is a hint that still processes similar to Langmuir kinetics are involved, that however, hydration water, Brownian mobility and steric processes prevent a closer packing.

2.4. In vitro drug release

The desorption of ASB from the PBCA NPs in different media (TRIS buffer pH 7.4 and human serum) was compared to that in purified water (MilliQ) (Fig. 6). As phosphate is a competitive inhibitor of ASB, TRIS buffer was used instead of phosphate buffer. In the latter, after 60 min 32 % and in human blood serum 30 % of the adsorbed ASB was released. In both cases, considerable desorption took place immediately after dilution again being indicative of Langmuir kinetics. The burst release in serum amounted to 22 % of the adsorbed ASB. Based on the results of the previous experiments, these data suggest that the stability of the formulation in blood serum may be sufficient for a delivery of the ASB to the brain. Indeed, as shown by transmission electron microscopy (TEM) of mice brain tissue, the nanoparticles made of human serum albumin (HSA) were visible in the neurons already 30 min after intravenous administration (Zensi et al. 2009).

2.5. Conclusions

These experiments demonstrate that large enzymes such as ASB can be efficiently be bound to poly(butyl cyanoacrylate) (PBCA) nanoparticles. It is very likely that other LSD enzymes also can be bound in a similar way. This would open up new possibilities for the treatment of other diseases like Fabry, metachromatic leucodystrophy, and others.

3. Experimental

3.1. Chemicals

Arylsulfatase B (*N*-acetylgalactosamine-4-sulfate sulfatase, Naglazyme® 1 mg/ml) from BioMarin Europe Limited, Novato, CA, USA; n-butyl-(2)-cyanoacrylate (Sicomet®) from Sichel-Werke, Hannover, Germany; 0.1 N hydrochloric acid and 1N sodium hydroxide from VWR, Darmstadt, Germany; Dextran 70000, p-nitrocatechol sulphate (pNCS) and human serum albumin (HSA) were from Sigma, St. Louis, MO, USA; hydroxymethylaminomethane (TRIS) from Molekula, Gillingham, UK; other chemicals were of analytical grade.

3.2. Nanoparticle preparation

The PBCA nanoparticles were prepared by anionic polymerisation, as described previously (Couvreur et al. 1979): 1 % of n-butyl-(2)-cyanoacrylate was added to a 1 % dextran 70000 solution in 0.01 N HCl with

Table 3: List of the adsorption parameters and their variations

Varied parameters Type	Variation
Temperature (°C)	4; 20
pH	4.5; 5.5; 6.3; 7.3
Induced ASB concentration [mg/ml]	1.0; 1.5; 2.0; 2.5; 3.0
Incubation time (h)	1, 2, 4, 6, 24

constant stirring. Stirring was continued for 2.5 h, subsequently the polymerisation was completed by neutralisation with 0.1 N NaOH. The mixture was filtered through a G2 sintered glass filter (Schott, Mainz, Germany) with a pore size of 40 – 100 μm to remove agglomerates and then lyophilised with 3 % mannitol as lyoprotector.

3.3. Determination of particle yield

Particle content was determined by gas chromatography (GC), as described by Langer et al. (1994). For this purpose, PBCA NPs were hydrolysed for 12 h with 2 N sodium hydroxide solution, and free butanol formed upon hydrolysis was extracted with dichloromethane. The sample (1 μl) was injected into the GC system (Hewlett-Packard 5890 Series II), and the concentration of butanol using pentanol as internal standard was measured. The particle yield was calculated as mg butyl-cyanoacrylate per ml suspension.

3.4. Adsorption of ASB to the PBCA nanoparticle surface

In order to determine the ASA adsorption to the PBCA nanoparticles, the freeze-dried particles were resuspended in aqueous solutions using ASB concentrations in the range of 1 – 3 mg/ml at different pH values ranging from 4.5 to 7.3, temperatures of 4 °C and 20 °C, and different stirring times (650 rpm, Thermomix, Germany). A list of the varied parameters is given in Table 3. After incubation, the particles were separated by centrifugation (30 min, 20'000 g; Eppendorf, Germany); the supernatant was carefully removed and analysed.

3.5. Drug loading: ASB quantification by size exclusion chromatography (SEC) and enzyme activity assay

The ASB activity assay was performed as described earlier (Baum et al. 1959), using p-nitrocatechol sulphate (pNCS) as a substrate. A 10 mM pNCS solution was added to the diluted samples and incubated for 30 min at 37 °C under constant shaking (650 rpm, Thermomix, Germany). The reaction was terminated by addition of 200 μl of a 1 N sodium hydroxide solution. The absorption of the resulting 4-nitroquinone was measured at 515 nm (U-3000 spectrometer, Hitachi Ltd., Tokyo, Japan).
The nanoparticles were removed by centrifugation (20'000 g; 30 min), the supernatants were carefully separated, and the amount of free enzyme was measured by size exclusion chromatography (SEC) (Merck Hitachi). A Shodex Protein 800 KW column (Shodex, Japan) was used as a stationary phase. The ASB was detected using a spectrophotometric detector at 280 nm using a phosphate buffer (pH 6.6) as eluent. The ASB content was calculated using a calibration curve, and the amount of adsorbed ASB was determined indirectly using Eq. (4):

$$Drug\ loading\,[\%] = \frac{m\,(total\ drug) - m(free\ drug)}{m(total\ drug)} 100 \qquad (4)$$

3.6. Measurements of particle size and zeta-potential

The resulting nanoparticles were characterised regarding mean diameter, polydisper sity, and particle zeta potential by photon correlation spectroscopy (PCS) in water using a Nanosizer ZS (Malvern Instruments Ltd., Malvern, UK). The samples were diluted 1:50 with purified water, the temperature was set to 25 °C, and the particle size was measured at a scattering angle of 173°. The zeta potential was measured likewise using a palladium electrode dip cell.

3.7. Scanning electron microscopy

The particle morphology was investigated by scanning electron microscopy (SEM Hitachi S-4500). For this purpose, the nanoparticle suspension was applied to an aluminum sample plate and dried overnight at ambient temperature. To obtain electrical conductibility, the particles were sputtered with gold for 70 s under argon atmosphere. Afterwards the samples were analysed at 25 kV with an upper detector. Digital pictures were taken with the Digital Image Processing System (Point Electronic, Halle, Germany).

3.8. Adsorption isotherm model fitting

The relationship between ASB concentration and sorption process can be analysed by the mathematically linearised models of Langmuir and Freundlich. The data were fitted to either the Freundlich or the Langmuir isotherm by regression curve analysis and determination of the respective correlation coefficients.

3.9. In vitro release kinetics

The *in vitro* release of loaded ASB from the nanoparticles was monitored after using the dilution centrifugation method. The ASB-loaded nanoparticles in suspension were diluted 10-fold with either MilliQ water, or TRIS buffer (pH 7.4), or human blood serum. The samples were analysed after 5, 20, and 60 min as well as immediately after dilution. The released enzyme was separated from the NP by centrifugation (30 min, 20000 g). The obtained supernatant was analysed by the activity assay described above. The percentage of release was calculated by subtracting the released ASB concentration from the enzyme concentration found in MilliQ control divided by the initial ASB concentration. Equation (5) was used:

$$release\,[\%] = \frac{m_t - m_{MQt}}{m_0} \cdot 100 \qquad (5)$$

where m_t is the mass of ASB in the eluent at the time [μg], m_{MQt} the mass of ASB in MilliQ at the time [μg], and m_0 the initial mass of ASB [μg].

Acknowledgements: This study was supported by a grant of the Brains for Brain (B4B) Foundation, Padova, Italy. The authors also would like to thank Prof. M. Beck from the Childrenĭs hospital, Gutenberg University Mainz, Germany for ASB.

References

Agogbua SI, Wynn CH (1976) Purification and properties of arylsulphatase B of human liver. Biochem J 153: 415–421.

Alyautdin RN, Petrov VE, Langer K, Berthold A, Kharkevich DA, Kreuter J (1997) Delivery of loperamide across the blood-brain barrier with polysorbate 80-coated polybutylcyano acrylate nanoparticles. Pharm Res 14: 325–328.

Alyautdin RN, Tezikov EB, Ramge P, Kharkevich DA, Begley DJ, Kreuter J (1998) Significant entry of tubocurarine into the brain of rats by adsorption to polysorbate 80-coated polybutylcyanoacrylate nanoparticles: an *in situ* brain perfusion study. J Microencapsul 15: 67–74.

Auclair D, Finnie J, White J, Nielsen T, Fuller M, Kakkis E, Cheng A, O'Neill CA, Hopwood JJ (2010) Repeated intrathecal injections of recombinant human 4-sulphatase remove dural storage in mature mucopolysaccharidosis VI cats primed with a short-course tolerisation regimen. Mol Genet Metab 99: 132–141.

Auclair D, Finnie J, Walkley SU, White J, Nielsen T, Fuller M, Cheng A, O'Neill CA, Hopwood JJ (2012) Intrathecal recombinant human 4-sulfatase reduces accumulation of glycosaminoglycans in dura of mucopolysaccharidosis VI cats. Pediatr Res 71: 39–45.

Baum H, Dodgson KS, Spencer B (1959) The assay of arylsulphatases A and B in human urine. Clin Chim Acta 4: 453–455.

Blanco MD, Alonso MJ (1997) Development and characterization of protein-loaded poly (lactide-co-glycolide) nanospheres. Eur J Pharm Biopharm 43: 287–294.

Couvreur P, Kante B, Roland M, Guiot P, Bauduin P, Speiser P (1979) Polycyanoacrylate nanocapsules as potential lysosomotropic carriers: preparation, morphological and sorptive properties. J Pharm Pharmacol 31: 331–332.

Fuller M, Brooks DA, Evangelista M, Hein LK, Hopwood JJ, Meikle PJ (2005) Prediction of neuropathology in mucopolysaccharidosis I patients. Mol Genet Metab 84: 18–24.

Gibson GJ, Saccone GT, Brooks DA, Clements PR, Hopwood JJ (1987) Human N-acetylgalactosamine-4-sulphate sulphatase. Purification, monoclonal antibody production and native and subunit Mr values. Biochem J 248: 755–764.

Kakkis E, McEntee M, Vogler C, Le S, Levy B, Belichenko P, Mobley W, Dickson P, Hanson S, Passage M (2004) Intrathecal enzyme replacement therapy reduces lysosomal storage in the brain and meninges of the canine model of MPS I. Mol Genet Metab 83: 163–174.

Kreuter J (1983) Physicochemical characterization of polyacrylic nanoparticles. Int J Pharm 14: 43–58.

Kreuter J, Alyautdin RN, Kharkevich DA, Ivanov AA (1995) Passage of peptides through the blood-brain barrier with colloidal polymer particles (nanoparticles). Brain Res 674: 171–174.

Kreuter J, Shamenkov D, Petrov V, Ramge P, Cychutek K, Koch-Brandt C, Alyautdin R (2002) Apolipoprotein-mediated transport of nanoparticle-bound drugs across the blood-brain barrier. J Drug Target 10: 317–325.

Kurakhmaeva KB, Djindjikhashvili IA, Petrov VE, Balabanyan VU, Voronina TA, Trofimov SS, Kreuter J, Gelperina S, Begley D, Alyautdin RN (2009) Brain targeting of nerve growth factor using poly(butyl cyanoacrylate) nanoparticles. J Drug Target 17: 564–574.

Langer K, Seegmüller E, Zimmer A, Kreuter J (1994) Characterisation of polybutylcyanoarylate nanoparticles: I. Quantification of PCBA polymer and dextrans. Int J Pharm 110: 21–27.

Langmuir I (1916) The constitution and fundamental properties of solids and liquids. Part I. Solids. J Am Chem Soc 38: 2221–2295.

Lukatela G, Krauss N, Theis K, Selmer T, Gieselmann V, von Figura K, Saenger W (1998) Crystal structure of human arylsulfatase A: the aldehyde function and the metal ion at the active site suggest a novel mechanism for sulfate ester hydrolysis. Biochemistry 37: 3654–3664.

Michaelis K, Hoffmann MM, Dreis S, Herbert E, Alyautdin RN, Michaelis M, Kreuter J, Langer K (2006) Covalent linkage of apolipoprotein e to albumin nanoparticles strongly enhances drug transport into the brain. J Pharmacol Exp Ther 317: 1246–1253.

Nonckreman CJ, Fleith S, Rouxhet PG, Dupont-Gillain CC (2010) Competitive adsorption of fibrinogen and albumin and blood platelet adhesion on surfaces modified with nanoparticles and/or PEO. Colloids Surf B Biointerfaces 77: 139–149.

Richardson NE, Meakin BJ (1974) The sorption of benzocaine from aqueous solution by nylon 6 powder. J Pharm Pharmacol 26: 166–174.

Salerno M, Cenni E, Fotia C, Avnet S, Granchi D, Castelli F, Micieli D, Pignatello R, Capulli M, Rucci N, Angelucci A, Del Fattore A, Teti A, Zini N, Giunti A, Baldini N (2010) Bone-targeted doxorubicin-loaded nanoparticles as a tool for the treatment of skeletal metastases. Curr Cancer Drug Targets 10: 649–659.

Steiniger SCJ, Kreuter J, Khalansky AS, Skidan IN, Bobruskin AI, Smirnova ZS, Severin SE, Uhl R, Kock M, Geiger KD, Gelperina SE (2004) Chemotherapy of glioblastoma in rats using doxorubicin-loaded nanoparticles. Int J Cancer 109: 759–767.

Wang Y, Hanson M (1988) Formulations of proteins and peptides: stability and stabilizers. J. Parenter. Sci. Technol. 42: 3–26.

Wraith JE (2006) Limitations of enzyme replacement therapy: current and future. J Inherit Metab Dis 29: 442–447.

Yaghootfam A, Schestag F, Dierks T, Gieselmann V (2003) Recognition of arylsulfatase A and B by the UDP-N-acetylglucosamine:lysosomal enzyme N-acetylglucosamine-phosphotransferase. J Biol Chem 278: 32653–32661.

Zensi A, Begley D, Pontikis C, Legros C, Mihoreanu L, Wagner S, Buchel C, von Briesen H, Kreuter J (2009) Albumin nanoparticles targeted with Apo E enter the CNS by transcytosis and are delivered to neurones. J Control Release 137: 78–86.